ICMIEE-PI-140102

Effect of Prandtl Number on 3D Heat Transfer through a Solar Collector

Rehena Nasrin, Salma Parvin and M.A. Alim*

Department of Mathematics, Bangladesh University of Engineering and Technology
Dhaka-1000, Bangladesh

ABSTRACT

Solar water heating systems are useful most likely to be cost effective for facilities with water heating systems that are expensive to operate or with operations such as laundries or kitchens that require large quantities of hot water. While solar collectors are most cost-effective in sunny, temperate areas, they can be cost effective virtually anywhere in the country so should be considered. Solar energy is one of the best sources of renewable energy with minimal environmental impact. The forced convection in solar collector continues to be a very active area of research during the past few decades. Commercial applications of solar collectors include swimming pool, space heating, car washes, military laundry facilities and eating establishments. A 3D heat transfer model is developed in which direct sunlight is incident on transparent glass cover of a flat plate solar collector (FPSC). Water/copper nanofluid is considered as heat transfer medium through the flat plate solar collector. The governing partial differential equations are solved using finite element method with Galerkin's weighted residual technique. In order to evaluate the temperature profile within the collector, the mass and momentum balance equations and heat transport equations for solid and fluid are solved numerically. Effect of Prandtl number is shown graphically in terms of streamlines pattern, rate of heat transfer (Nu), average temperature (θ_{av}), percentage of collector efficiency (η), outlet temperature (T) for water-Cu nanofluid and base fluid (clear water) through the collector. It is observed that at the highest value of Prandtl number the water based nanofluid is more effective than base fluid for the enhancement of heat transfer rate and collector efficiency.

Keywords: 3D heat transfer, flat plate solar collector, finite element method, Prandtl number, forced convection.

1. Introduction

Solar flat plate collectors are commonly used for domestic and industrial purposes and have the largest commercial application amongst the various solar collectors. This is mainly due to simple design as well as low maintenance cost. Solar radiation is radiant energy emitted by the sun. It is particularly electromagnetic energy. Solar irradiance (I) is the combination of bright light and radiant heat. Heat transfer due to emission of electromagnetic waves is known as thermal radiation. The heat transfer rate per unit area as thermal radiation is called radiative heat flux.

The fluids with solid-sized nanoparticles suspended in them are called "nanofluids". Applications of nanoparticles in thermal field are to augment warmth transport from solar collectors to luggage compartment tanks, to pick up proficiency of coolants in transformers.

The absorptance of the collector surface for shortwave solar radiation depends on the nature and colour of the coating and on the incident angle. Usually black colour is used. Various colour coatings had been proposed by Wazwaz et al. [1] mainly for aesthetic reasons. A low-cost mechanically manufactured selective solar absorber surface method had been proposed by Konttinen et al. [2]. A numerical experiment is performed for inclined solar collectors by Varol and Oztop [3]. Results indicated that heat transfer was increased with increasing Rayleigh number and aspect ratio, and was decreased with increasing wavelength.

There are so many methods introduced to increase the efficiency of the solar water heater of Xiaowu and Hua [4] and Hussain [5]. Hwang et al. [6] performed stability and thermal conductivity characteristics of nanofluids. In this study, they concluded that the thermal conductivity of ethylene glycol was increased by 30%.

Karanth et al. [7] numerically simulated a solar flat plate collector using Discrete Transfer Radiation Model. A 3D model of the collector involving the water pipe, absorber plate, the glass top and the air gap in-between the absorber plate and the glass top was modeled to provide for conduction, convection and radiation in their analysis. Bég et al. [8] performed non-similar mixed convection heat and species transfer along an inclined solar energy collector surface with cross diffusion effects, where the resulting governing equations were transformed and then solved numerically using the local nonsimilarity method and Runge-Kutta shooting quadrature. Manjunath et al. [9] analyzed three

* Corresponding author. Tel.: +88-01766924295
E-mail address: rehena@math.buet.ac.bd

dimensional conjugate heat transfers through unglazed solar flat plate collector. They used finned tubes and the heat transfer simulation due to solar irradiation to the fluid medium, increased with an increase in the mass flow rate. Vestlund [10] studied gas-filled flat plate solar collector. The gases examined were argon, krypton and xenon in his thesis paper.

Manjunath et al. [11] studied comparatively solar dimple plate collector with flat plate collector to augment the thermal performance. Their result described that the average exit water temperature showed a marked improvement of about 5.5^0C for a dimple solar collector as compared to that of a flat plate solar collector. CFD analysis of solar flat plate collector was conducted by Ingle et al. [12]. His work attempted to present numerical simulation of solar collector developed exclusively for grape drying. CFD analysis of triangular absorber tube of a solar flat plate collector was performed by Basavanna and Shashishekar [13] where the numerical results obtained using the experimentally measured temperatures are compared to the temperatures determined by the CFD model. Tagliafico et al. [14] reviewed dynamic thermal models and CFD analysis for flat-plate thermal solar collectors. A review of solar collector models was presented, including a proper classification and a description of main characteristics and performances in their study. Nasrin and Alim [15] developed a semi-empirical relation for forced convective analysis through a solar collector. A new correlation was derived from their obtained results and it was easy to use heat transfer purposes.

From the above literature review it is mentioned that a very few 3D numerical studies have been completed using traditional fluid that is water, gas, air etc. Thus there is a large scope to work 3D numerical investigation of heat transfer through a flat plate solar collector using nanofluid.

2. Problem Formulation

A schematic diagram of the system in three dimensional as well as cross sectional view considered in the present study is shown in Fig. 1. The system consists of a flat plate solar collector. The working fluid in the collector is water-based nanofluid containing Cu nanoparticles. The nanoparticles are generally spherical shaped and diameter is taken as 5 nm. The nanofluid is considered as single phase flow and surfactant analysis is neglected. The solar collector is a metal box with highly transparent and anti-reflected glass cover (called the glazing) on top and a dark colored copper absorber plate on the bottom. Length, width and thickness of the absorber plate are 1m, 0.15m and 0.0008m respectively. The riser pipe has inner diameter 0.01 m and thickness 0.0005m. Coefficients of heat absorption and emmision of copper absorber are 95% and 5% respectively. A trapezium shaped bonding conductance is located from middle one-third part of width of the absorber plate. It covers the three-fourth part of the riser pipe. It is as long as the absorber plate and tube. The bonding conductance is made of copper metal. The computation domain is the copper absorber plate containing a fluid passing copper riser pipe with bonding conductance. The riser pipe is generally ultrasonically welded to the absorber plate.

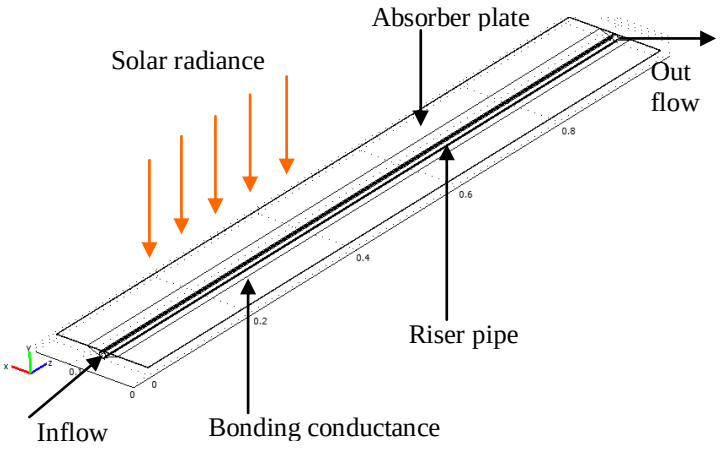

Fig. 1: Schematic diagram of the flat plate solar collector

3. Mathematical Formulation

In the present problem, it can be considered that the flow is three-dimensional and there is no viscous dissipation. The nanofluid is assumed incompressible and the flow is considered to be laminar. It is taken that water and nanoparticles are in thermal equilibrium and no slip occurs between them. Only steady state case is considered. The 3D governing equations in dimensional form are as follows

$$\frac{\partial u}{\partial x}+\frac{\partial v}{\partial y}+\frac{\partial w}{\partial z}=0$$

$$\rho_{nf}\left(u\frac{\partial u}{\partial x}+v\frac{\partial u}{\partial y}+w\frac{\partial u}{\partial z}\right)=-\frac{\partial p}{\partial x}+\mu_{nf}\left(\frac{\partial^2 u}{\partial x^2}+\frac{\partial^2 u}{\partial y^2}+\frac{\partial^2 u}{\partial z^2}\right)$$

$$\rho_{nf}\left(u\frac{\partial v}{\partial x}+v\frac{\partial v}{\partial y}+w\frac{\partial v}{\partial z}\right)=-\frac{\partial p}{\partial y}+\mu_{nf}\left(\frac{\partial^2 v}{\partial x^2}+\frac{\partial^2 v}{\partial y^2}+\frac{\partial^2 v}{\partial z^2}\right)$$

$$\rho_{nf}\left(u\frac{\partial w}{\partial x}+v\frac{\partial w}{\partial y}+w\frac{\partial w}{\partial z}\right)=-\frac{\partial p}{\partial z}+\mu_{nf}\left(\frac{\partial^2 w}{\partial x^2}+\frac{\partial^2 w}{\partial y^2}+\frac{\partial^2 w}{\partial z^2}\right)$$

$$u\frac{\partial T}{\partial x}+v\frac{\partial T}{\partial y}+w\frac{\partial T}{\partial z}=\alpha_{nf}\left(\frac{\partial^2 T}{\partial x^2}+\frac{\partial^2 T}{\partial y^2}+\frac{\partial^2 T}{\partial z^2}\right)$$

$$\frac{k_a}{\rho C_p}\left(\frac{\partial^2 T_a}{\partial x^2}+\frac{\partial^2 T_a}{\partial y^2}+\frac{\partial^2 T_a}{\partial z^2}\right)=0$$

where, $\alpha_{nf}=k_{nf}/\left(\rho C_p\right)_{nf}$ is the thermal diffusivity, $\rho_{nf}=(1-\phi)\rho_f+\phi\rho_s$ is the density, $\left(\rho C_p\right)_{nf}=(1-\phi)\left(\rho C_p\right)_f+\phi\left(\rho C_p\right)_s$ is the heat capacitance, $\mu_{nf}=\dfrac{\mu_f}{(1-\varphi)^{2.5}}$ is the viscosity of

Brinkman Model [16], the thermal conductivity of Maxwell Garnett (MG) model [17] is

$$k_{nf} = k_f \frac{k_s + 2k_f - 2\phi\left(k_f - k_s\right)}{k_s + 2k_f + \phi\left(k_f - k_s\right)}$$

The boundary conditions of the computation domain are:

at all solid boundaries of the riser pipe: $u = v = w = 0$

at the solid-fluid interface: $k_f\left(\frac{\partial T}{\partial n}\right)_{fluid} = k_a\left(\frac{\partial T}{\partial n}\right)_{solid}$

at the inlet boundary of the riser pipe: $T = T_{in}$, $w = W_{in}$

at the outlet boundary: convective boundary condition $p = 0$

at the top surface of the absorber: heat flux $-k_a \frac{\partial T_a}{\partial z} = q = I\tau\kappa - U_L\left(T_{in} - T_{amb}\right)$

at the other surfaces of absorber plate: $\frac{\partial T_a}{\partial n} = 0$

at the outer boundary of riser pipe: $\frac{\partial T}{\partial n} = 0$

at the outer boundary of bonding conductance: $\frac{\partial T_a}{\partial n} = 0$

The governing equations are non-dimensionalized by using the following dimensionless quantities

$$X = \frac{x}{D},\ Y = \frac{y}{D},\ Z = \frac{z}{D},\ U = \frac{u}{W_{in}},\ V = \frac{v}{W_{in}},\ W = \frac{w}{W_{in}},$$

$$P = \frac{p}{\rho_f {U_{in}}^2},\ \theta = \frac{\left(T - T_{in}\right)k_f}{qL},\ \ \theta_a = \frac{\left(T_a - T_{in}\right)k_a}{qL}$$

and $Pr = \frac{\nu_f}{\alpha_f}$ is the Prandtl number, $K = \frac{k_a}{k_f}$ is thermal conductivity ratio, $Re = \frac{W_{in} D}{\nu_f}$ is the Reynolds number, n and N is the dimensional and non-dimensional distances either along x or y or z directions acting normal to the surface respectively.

The average heat transfer rate of the collector can be written as

$$Nu = \frac{\iint_S \overline{Nu}\, ds}{\iint_s dS} = -\frac{1}{\pi DL}\frac{k_{nf}}{k_f}\iint_S \sqrt{\frac{\partial^2\theta}{\partial X^2} + \frac{\partial^2\theta}{\partial Y^2} + \frac{\partial^2\theta}{\partial Z^2}}\, ds$$

where L is the height of absorber tube.

The mean bulk temperature and average sub domain velocity of the fluid inside the collector may be written as $\theta_{av} = \frac{\iiint_v \theta d\mathrm{V}}{\iiint_v d\mathrm{V}} = \frac{4}{\pi D^2 L}\iiint_v \theta d\mathrm{V}$ and

$$\overline{\mathrm{V}}_{av} = \frac{\iiint_v \overline{\mathrm{V}} d\mathrm{V}}{\iiint_v d\mathrm{V}} = \frac{4}{\pi D^2 L}\iiint_v \overline{\mathrm{V}}\, d\mathrm{V} \quad , \text{ where V is the volume the absorber tube.} \qquad (17)$$

A measure of a flat plate collector performance is the collector efficiency (η) defined as the ratio of the useful energy gain (Q_{usfl}) to the incident solar energy. The instantaneous thermal efficiency of the collector is:

$$\eta = \frac{\text{useful gain}}{\text{available energy}} = \frac{Q_{\text{usfl}}}{AI} = \frac{F_R A\left[I\left(\tau\kappa\right) - U_L\left(T_{in} - T_{amb}\right)\right]}{AI}$$

$$= F_R\left(\tau\kappa\right) - F_R U_L \frac{\left(T_{in} - T_{amb}\right)}{I}$$

4. Numerical Formulation

The Galerkin finite element method Taylor and Hood [18] and Dechaumphai [19] is used to solve the non-dimensional governing equations along with boundary conditions for the considered problem. Conservation equations are solved for the finite element method to yield the velocity and temperature fields for the water flow in the absorber tube and the temperature fields for the absorber plate. The equation of continuity has been used as a constraint due to mass conservation and this restriction may be used to find the pressure distribution. The penalty finite element method is used to solve the governing equations, where the pressure P is eliminated by a penalty constraint. The continuity equation is automatically fulfilled for large values of this penalty constraint. Then the velocity components (U, V, W) and temperatures (θ, θ_a) are expanded using a basis set. The Galerkin finite element technique yields the subsequent nonlinear residual equations. Gaussian quadrature technique is used to evaluate the integrals in these equations. The non-linear residual equations are solved using Newton–Raphson method to determine the coefficients of the expansions. The convergence of solutions is assumed when the relative error for each variable between consecutive iterations is recorded below the convergence criterion such that $\left|\psi^{n+1} - \psi^n\right| \le 1.0\text{e}^{-6}$, where n is the number of iteration and Ψ is a function of U, V, W, θ and θ_a.

4.1 Mesh Generation

In finite element method, the mesh generation is the technique to subdivide a domain into a set of sub-domains, called finite elements, control volume etc. The discrete locations are defined by the numerical grid, at which the variables are to be calculated. It is basically a discrete representation of the geometric domain on which the problem is to be solved. The computational domains with irregular geometries by a collection of finite elements make the method a valuable practical tool for the solution of boundary value problems arising in various fields of engineering. Fig. 2 displays the 3D finite element mesh of the present physical domain. Fine mesh size is chosen for this geometry. The thermo-

physical properties of water and nanoparticles are taken from Ogut [20] and given in Table 1.

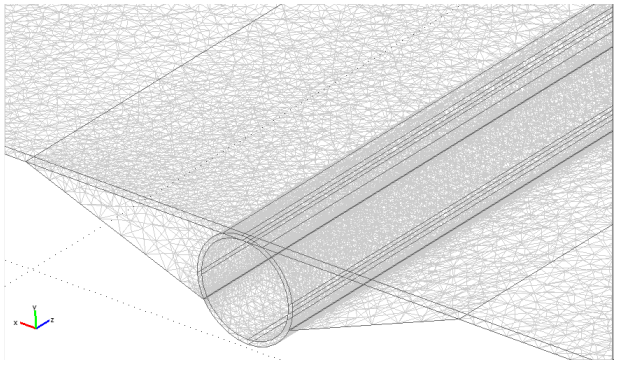

Fig. 2: Mesh generation of the collector

Table 1: Thermo-physical properties of water and Cu nanoparticles at 295K

Physical Properties	Fluid phase (water)	Cu
C_p(J/kgK)	4181	385
ρ (kg/m^3)	998.0	8933
k (W/mK)	0.606	400
$\alpha\times10^7$ (m^2/s)	1.47	1163.1
$\mu\times10^6$ (Ns/ m^2)	959	-

4.2. Grid Independent Test

The arrangement of discrete points throughout the domain is simply called a grid. The determination of a proper grid for the flow through a given geometric shape is important. The way that such a grid is determined is called grid generation. The grid generation is a significant consideration in CFD. Finite element method can be applied to unstructured grids. This is because the governing equations in this method are written in integral form and numerical integration can be carried out directly on the unstructured grid domain in which no coordinate transformation is required. The three dimensional computational domain is modeled using finite element mesh as shown in Fig. 2. The complete domain consists of 14,20,465 elements which include the riser tube and absorber plate. The mesh is composed of tetrahedron element type with ten nodes. The grid independence test is performed to check validity of the quality of mesh on the solution. The influence of further refinement does not change the result by more than 1.25 % which is taken here as the appropriate mesh quality for computation.

5. Results and Discussion

Finite element simulation is applied to perform the analysis of laminar forced convection temperature and fluid flow through a riser pipe of a flat plate solar collector filled with water/copper nanofluid. Effect of the Prandtl number (Pr) on heat transfer and collector efficiency of solar collector has been studied. The values of Prandtl number are taken as 4.2, 5.2, 6.6 and 7.6. All values chosen for the Prandtl number represent water at different temperature. Solid volume fraction (ϕ) is assumed to be fixed at 2%.

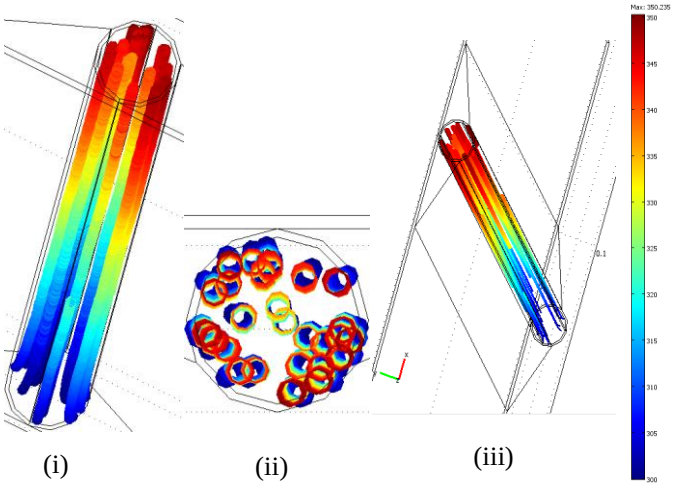

(i) (ii) (iii)

Fig. 3: Streamline plot with color expression for temperature (i) front view, (ii) slide view and (iii) back view

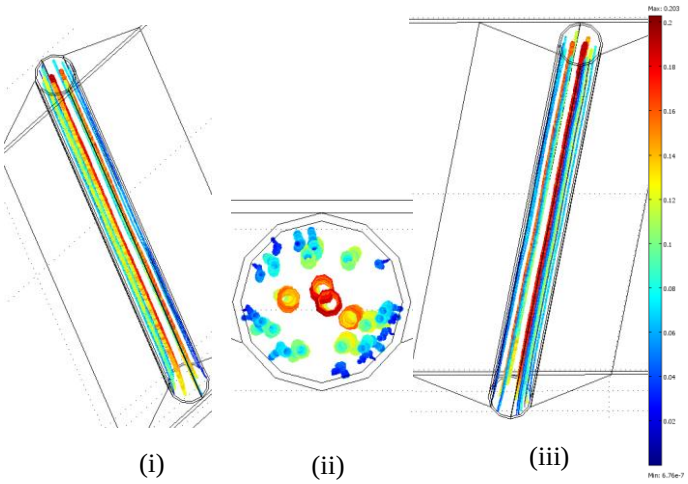

(i) (ii) (iii)

Fig. 4: Streamline plots with color expression for velocity (i) Front view, (ii) slide view and (iii) back view

Fig. 3(i-iii) represents the streamlines plot with color expression for temperature at Re = 1000, Pr = 6.6 and ϕ = 2%. The different colours indicate different temperature of streamlines. Streamlines plot are shown as front view, slide view and back view of a collector for water-copper nanofluid. The streamlines occupying the whole riser pipe of the flat plate solar collector. In all views of streamlines it is observed that the flow is laminar and the streamlines are parallel to each other. The temperature of the streamlines which are closer to the solid pipe is higher than the lines at the middle of the pipe.

On the other hand the streamlines plot with color expression for velocity field is shown in Fig. 4(i-iii). The strength of the streamlines which are closer to the solid pipe is lower than the lines at the middle of the pipe. That is the practical phenomena of the solar collector are satisfied by this simulation.

The average Nusselt number (*Nu*), average temperature (θ_{av}), collector efficiency (η), outlet mean temperature (dimensional) of nanofluid, subdomain mean velocity along with the various Prandtl number (*Pr*) are displayed in Fig. 5 (i)-(v). *Nu* enhances sharply with growing *Pr*. The rate of heat transfer for water-copper nanofluid is found to be more effective than the clear water due to higher thermal conductivity of solid nanoparticles. For growing viscous force from 4.2 to 7.6 rate of heat transfer rises 29% and 20% using water/Cu nanofluid and water respectively.

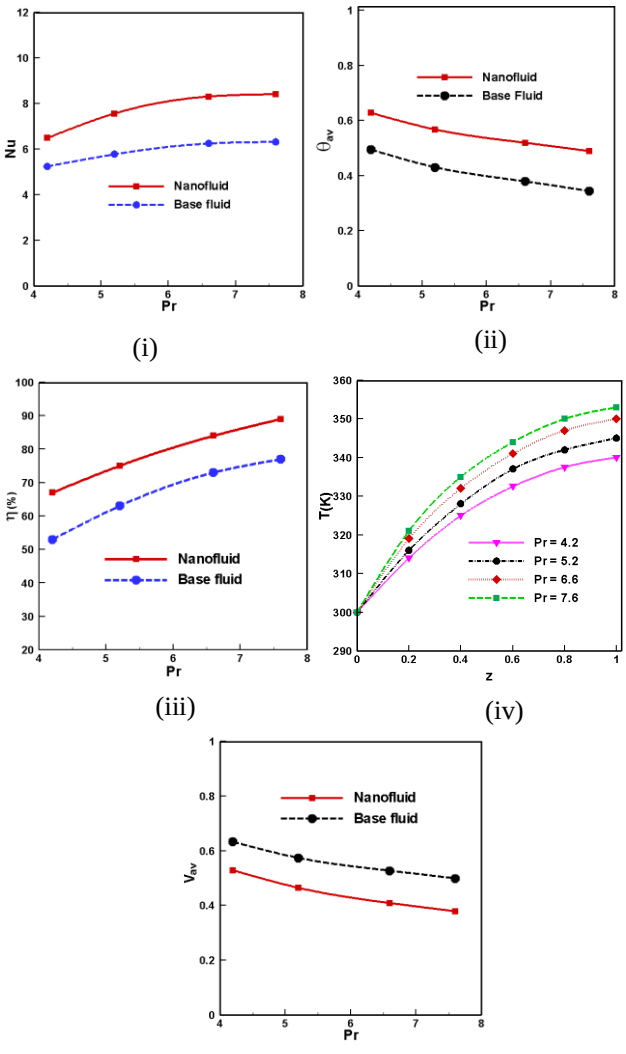

Fig. 5: Effect of *Pr* on (i) *Nu*, (ii) θ_{av}, (iii) η, (iv) *T* and (v) V

Mean temperature of fluids devalues gradually along with the increasing Prandtl numbers. It is well known that higher values of *Pr* indicate lower temperature of fluids. Here base fluid has lower mean temperature than the water-Cu nanofluid.

From Fig. 5(iii) it is observed that decreasing *Pr* devalues the percentage of collector efficiency (η) because greater *Pr* represents low tempered water which is found in winter season. Temperature of output water becomes high in summer season. Thermal efficiency enhances from 67%-89% for nanofluid and 53%-77% for water.

The inlet temperature of water-Cu nanofluid is maintained at 300K and then it increases gradually with the contact of heated solid surfaces of the riser pipe. And finally the output mean temperature of nanofluid becomes 340K, 345K, 350K and 353K for *Pr* = 4.2, 5.2, 6.6 and 7.6 respectively.

Magnitude of mean velocity (V_{av}) has notable changes with different values of viscous forces. It is well known that velocity of higher viscous fluid is less than that of lower viscous fluid. Clear water moves freely than solid concentrated nanofluid. Falling viscous force enhance the mean velocity of the fluids through the riser pipe of the flat plate solar collector.

6. Conclusion

Following conclusions have been drawn from the results of the numerical analysis:

- The configuration of the streamlines plot of heat and flow fields of the solar flat plate collector is found to significantly depend upon *Pr*.
- The water-Cu nanofluid with the highest *Pr* is established to be most effective in enhancing performance of heat transfer rate.
- Mean temperature devalues for both fluids with growing values of *Pr*.
- Collector efficiency is obtained higher for the highest Prandtl number.
- Outlet temperature of nanofluid rises due to escalating *Pr*.

NOMENCLATURE

A	Surface area of solar flat plate collector (m^2)
C_p	Specific heat at constant pressure (J kg^{-1} K^{-1})
I	Intensity of solar radiation (W m^{-2})
k	Thermal conductivity (W m^{-1} K^{-1})
L	Length of the solar collector (m)
m	Mass flow rate (Kg s^{-1})
Nu	Nusselt number,
Pr	Prandtl number,
Re	Reynolds number
T	Dimensional temperature (K)
T_{in}	Input temperature of nanofluid (K)
T_{out}	Output temperature of fluid (K)
u, v, w	Dimensional *x, y* and *z* components of velocity (m s^{-1})
U_l	Local heat transfer coefficient (W m^{-2} K^{-1})
U_i	Input velocity of fluid (ms^{-1})
U, V, W	Non dimensional velocities
V	Volume of the absorber tube (m^3)
X, Y, Z	Non dimensional co-ordinates

x, y, z Dimensional co-ordinates (m)

Greek Symbols

α Fluid thermal diffusivity ($m^2\ s^{-1}$)

β Thermal expansion coefficient (K^{-1})

ϕ Nanoparticles volume fraction

ν Kinematic viscosity ($m^2\ s^{-1}$)

η Collector efficiency,

θ Dimensionless temperature,

ρ Density ($kg\ m^{-3}$)

μ Dynamic viscosity ($N\ s\ m^{-2}$)

Subscripts

a absorber

av mean

f fluid

nf nanofluid

s solid particle

usfl useful

REFERENCES

[1] J. Wazwaz, H. Salmi, R. Hallak, Solar thermal performance of a nickel-pigmented aluminium oxide selective absorber, *Renewable Energy*, Vol. 27, pp. 277–292, 2002.

[2] P. Konttinen, PD. Lund, RJ. Kilpi, Mechanically manufactured selective solar absorber surfaces, *Solar Energy Mater Solar Cells*, Vol. 79, No. 3, pp. 273–283, 2003.

[3] Y. Varol and HF. Oztop, Buoyancy induced heat transfer and fluid flow inside a tilled wavy solar collector, *Building Environment*, Vol. 42, pp. 2062-2071, 2007.

[4] W. Xiaowu, B. Hua, Energy analysis of domestic-scale solar water heaters, *Renew. Sustain Energy Rev.*, Vol. 9, No. 6, pp. 638–645, 2005.

[5] A. Hussain, The performance of a cylindrical solar water heater, *Renew. Energy*, Vol. 31, No. 11, pp. 1751–1763, 2006.

[6] Y. Hwang, JK. Lee, CH. Lee, YM. Jung, SI. Cheong, CG. Lee, BC. Ku, SP. Jang, Stability and thermal conductivity characteristics of nanofluids, *Thermochimica Acta*, Vol. 455, No. 1–2, pp. 70–74, 2007.

[7] K.V. Karanth, M.S. Manjunath, N.Y. Sharma, Numerical simulation of a solar flat plate collector using discrete transfer radiation model (DTRM) – a CFD approach, Proc. of the World Cong. on Engg., London, U.K., III, 2011.

[8] OA. Bég, A. Bakier, R. Prasad, SK. Ghosh, Numerical modelling of non-similar mixed convection heat and species transfer along an inclined solar energy collector surface with cross diffusion effects, *World J. of Mech.*, Vol. 1, pp. 185-196, 2011.

[9] M.S, Manjunath, K.V. Karanth, N.Y. Sharma, Three dimensional numerical analysis of conjugate heat transfer for enhancement of thermal performance using finned tubes in an economical unglazed solar flat plate collector, *Proc. of the World Cong. on Engg.*, London, U.K., III, 2011.

[10] J. Vestlund, Gas-filled, flat plate solar collector, Ph. D. Thesis, Building Services Engg., Dept. of Energy and Environ., Chalmers University of Technology, Gothenburg, Sweden, 2012.

[11] M.S, Manjunath, K.V. Karanth, N.Y. Sharma, A comparative CFD study on solar dimple plate collector with flat plate collector to augment the thermal performance, *World Academy of Sci., Engg. and Tech.*, Vol. 6, pp. 10-21, 2012.

[12] P.W. Ingle, A.A. Pawar, B.D. Deshmukh, K.C. Bhosale, CFD analysis of solar flat plate collector, *Int. J. of Emerg. Techn. and Adv. Engg.*, Vol. 3, No. 4, pp. 337-342, 2013.

[13] S., Basavanna and K.S. Shashishekar, CFD analysis of triangular absorber tube of a solar flat plate collector, *Int. J. Mech. Eng. & Rob. Res.*, Vol. 2, No. 1, pp. 19-24, 2013.

[14] I.A. Tagliafico, F. Scarpa, M.D. Rosa, Dynamic thermal models and CFD analysis for flat-plate thermal solar collectors –a review, *Renew. and Sust. Energy Rev.*, Vol. 2, No. 30, pp. 526-537, 2014.

[15] R. Nasrin and M.A. Alim, Semi-empirical relation for forced convective analysis through a solar collector, *Solar Energy*, Vol. 105, pp. 455-467, 2014.

[16] H.C. Brinkman, The viscosity of concentrated suspensions and solution, *Journal Chem. Physics*, Vol. 20, pp. 571–581, 1952.

[17] JC. Maxwell-Garnett, Colours in metal glasses and in metallic films, *Philos. Trans. Roy. Soc. A*, Vol. 203, pp. 385–420, 1904.

[18] C. Taylor, P. Hood, A numerical solution of the Navier-Stokes equations using finite element technique, *Computer and Fluids*, Vol. 1, pp. 73–89, 1973.

[19] P. Dechaumphai, Finite Element Method in Engineering, 2nd ed., *Chulalongkorn University Press, Bangkok*, 1999.

[20] EB. Ogut, Natural convection of water-based nanofluids in an inclined enclosure with a heat source, *Int. J. of Thermal Sciences*, Vol. 48, No. 11, pp. 2063-2073, 2009.